INVESTIGATION ON THE ORIGIN OF HIGH ENERGY X-RAYS OBSERVED IN THIRD GENERATION ECRIS

T. Thuillier*, LPSC, Grenoble, France

Abstract

The operation of third generation ECR ion source heated with 24 or 28 GHz microwave frequency shows a high energy x-ray spectrum with a characteristic temperature much higher than the one observed at the usual heating frequencies (14-18 GHz). The behaviour of the x-ray spectrum is studied based on the review of a set of data previously done at LBNL [1]. The data reviewed shows that the hot x-ray temperature scales with the ECR frequency. The experimental data is compared with the prediction of a simple model of ECR heating developed for this purpose. A formula to estimate the ECR resonance thickness is calculated. The model explains nicely the experimental x-ray temperature variation when the central magnetic field of the ECRIS is changed. It demonstrates that such a magnetic field variation does not change the electron confinement time and that the change of the x-ray spectrum temperature is due to the change of the ECR zone thickness. The only way for the model to reproduce the fact that the x-ray temperature scales with the ECR frequency is to assume that the electron confinement time scales (at least) with the ECR frequency. This result brings new credit to the theoretical prediction that the hot electron RF scattering is decreasing when the ECR frequency increases.[2,3] The spatial gyrac effect, which can be considered as another possible origin of the very hot x-ray produced in ECRIS is recalled for convenience in this paper.

VENUS EXPERIMENTAL DATA

Extensive experimental x-ray measurements have been carried out on several third generation ECR ion sources. This paper focuses on data formerly measured with the VENUS ion source at LBNL. [1] The data considered in this paper is the one comparing the x-ray spectrum produced at 18 GHz and 28 GHz with a homothetic magnetic field (*i.e.* scaling the ECR frequency) and for 2 values of the axial median magnetic field intensity (B_{min}):

- steep Gradient configuration when B_{min}~$0.47B_{ecr}$
- shallow Gradient configuration when B_{min}~$0.47B_{ecr}$

The axial magnetic field configuration associated to these four tuning is shown on Figure 1. The red and blue plots respectively stand for 28 and 18 GHz operation. Solid lines are for shallow gradient, while dashed lines are for steep gradient. The magnetic calculation have been carried out with RADIA.[4] The VENUS radial magnetic field is considered to reach 2.1 T at wall (radius 70 mm) for the 28 GHz operation and 1.35T for the 18 GHz operation.

The experimental x-ray spectrum plotted in [1] have been fitted with the usual Boltzmann temperature profile:

$$\frac{dN}{dE} \sim N_0 e^{-\frac{E}{kT}} \qquad (1)$$

The fits are plotted on Figure 2, and the spectrum temperatures calculated are summarized in the Table 1. The same convention of color and line style is used in Fig. 1 and 2 for convenience.

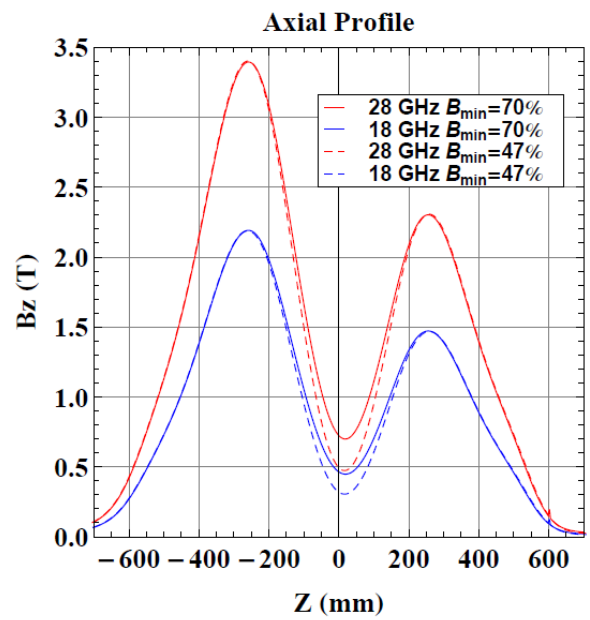

Figure 1: Axial magnetic field profiles used to study the x-ray spectrum dependence for 2 ECR frequencies and 2 B_{min} values.

Table 1: Experimental x-ray spectrum temperatures

f_{ECR}	Gradient type	kT
18 GHz	Steep	47.7 ± 2 keV
18 GHz	Shallow	91.2 ± 2 keV
28 GHz	Steep	72.7 ± 2 keV
28 GHz	Shallow	139.5 ± 2 keV

DATA ANALYSIS

A way to compare these spectrum is to normalize their values at the energy E=0 and consider that an individual x-ray population at a given dN/dE value undergoes an energy boost from E_1 to E_2 when the magnetic gradient changes from steep (kT_1) to shallow (kT_2), or when the frequency is changed from 18 to 28 GHz (with an appropriate homothetic magnetic field). This implies that:

*thuillier@lpsc.in2p3.fr

ISBN 978-3-95450-158-8

$$e^{-\frac{E_2}{kT_2}} = e^{-\frac{E_1}{kT_1}} \Rightarrow E_2 = \frac{kT_2}{kT_1} E_1 \qquad (2)$$

It is assumed next that when the magnetic gradient and/or the ECR frequency is changed, the plasma hot electron population undergoes an energy boost proportional to the x-ray temperature change. The experimental ratio of x-ray temperature between 28 and 18 GHz operation (for a homothetic magnetic field) and between shallow and steep gradients for a given ECR frequency are included in the Table 2. The experimental 28 to 18 GHz temperature ratio appears to be the same for the two gradients considered with a value of ~1.53. Since the ratio of the microwave frequencies 28 on 18 is 1.55, it is guessed that the hot x-ray temperature tail in an ECRIS is proportional to the microwave frequency (assuming a homothetic magnetic field configuration). A second interesting point comes from the fact that the shallow to steep gradient x-ray temperature ratio gives the same value for 18 GHz and 28 GHz. This time, the effect is expected to be due to the magnetic field.

Table 2: Experimental x-ray spectrum temperature ratios

f_{ECR}	Temperature ratio type	$\frac{kT_2}{kT_1}$
28/18 GHz	Shallow	1.52±0.11
28/18 GHz	Steep	1.53±0.06
18 GHz	Shallow /Steep	1.91±0.12
28 GHz	Shallow /Steep	1.92±0.08

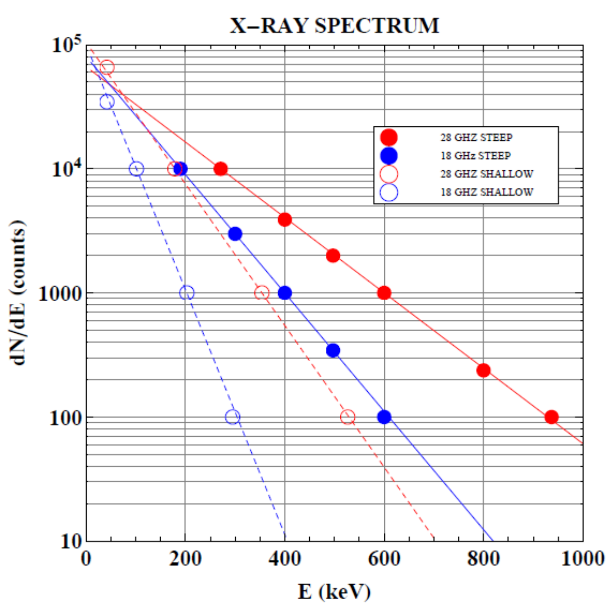

Figure 2: Fit of the x-ray spectrum extracted from [1]. Red curves are 28 GHz profiles. Blue curves are 18 GHz ones. Solid line are the "shallow" gradient tuning, dashed lines stand for "steep" gradient.

DISCUSSION

A higher temperature x-ray spectrum implies that the ion source generates much higher energy electrons. There are two obvious ways to increase the electron energy in an ECR ion source: either by increasing the electron confinement time or by increasing the mean energy gained when an electron passes through the ECR resonance area. This can be considered using a simple electron heating model:

$$W_\perp = \sum_{i=1}^{N} \epsilon_i \sim N\epsilon \qquad (3)$$

Where $W_\perp$ is the electron perpendicular energy, N is the electron mean number of passage through the ECR zone (before it is lost to the wall), and ϵ is the electron mean energy gained per passage. Thus, increasing the confinement time equals to increasing N which in turn increases $W_\perp$. This is the mechanism expected to occur using the hypothesis that the hot electron RF scattering phenomenon is decreasing when the ECR frequency increases. [3] Another way to explain a higher $W_\perp$ is to assume that $N \sim Constant$ and that instead ϵ increases. In this paper, we investigate the hypothesis that the electron energy could increase because of a change of the mean energy gain per passage ϵ through the ECR zone. To do so, a model to estimate ϵ is developed as a function of the ECR frequency.

ECR HEATING GAIN PER PASS

An estimate of an electron energy boost gained when crossing the ECR zone in a magnetic gradient is given by:

$$\epsilon \sim \frac{eE^2 \Delta t^2}{2m} \qquad (4)$$

Where e is the electron charge, E the local microwave field intensity, m the electron mass and Δt the time to cross the resonance. Δt is not a convenient parameter to estimate ϵ. One can define the ECR zone thickness $\Delta l = v_{||}\Delta t$ where $v_{||}$ is the electron velocity parallel to the magnetic field. But Δl still depends on the local magnetic field gradient intensity $g = \frac{\partial B}{\partial l}$, gradient taken along the local magnetic field line crossing the ECR zone. Δl can be substituted by $\frac{\Delta B}{g}$ where ΔB is the intrinsic ECR zone magnetic thickness. The ECR angular frequency ω is finally introduced in ϵ by considering that $\frac{\Delta B}{B} = \frac{\Delta\omega}{\omega}$. So the expression for ϵ becomes:

$$\epsilon \sim \frac{mE^2 \Delta\omega^2}{2e{v_{||}}^2 g^2} \qquad (5)$$

The question is now to estimate $\Delta\omega$ and study its possible dependences with physical parameters such as the ECR frequency ω_{ce} and the electrical field intensity E. This point is investigated in the next section.

ISBN 978-3-95450-158-8

ECR Peak Width Study

The intrinsic ECR thickness has been studied theoretically by solving the equation of motion (non-relativisitic cas) as a function of ω_{RF} , $\omega_{ce} = \frac{eB}{m}$ being considered constant:

$$\frac{d\vec{v}}{dt} = \frac{eE}{m} \cos \omega_{RF} t\, \vec{x} + \omega_{ce}\vec{z} \times \vec{v} \qquad (6)$$

The initial velocity considered is expressed as a function of a random phase angle ϕ: $\vec{v}(0) = v_0 \cos\phi \vec{x} + \sin\phi \vec{y}$ and the theoretical solution for the velocity is averaged on this angle. When $\omega_{RF} = \omega_{ce} + \Delta\omega$, an electron gains energy while $\Delta\omega \times t \leq \pi$. It then reaches an energy noted T_{max}. Next, the electron is out phased and eventually decelerates back to its initial velocity: the electron kinetic energy is thus increasing and decreasing periodically. This well-known effect [5] is shown on Fig. 3 for the particular case when $v_0 = 0$ for several values of $\Delta\omega$.

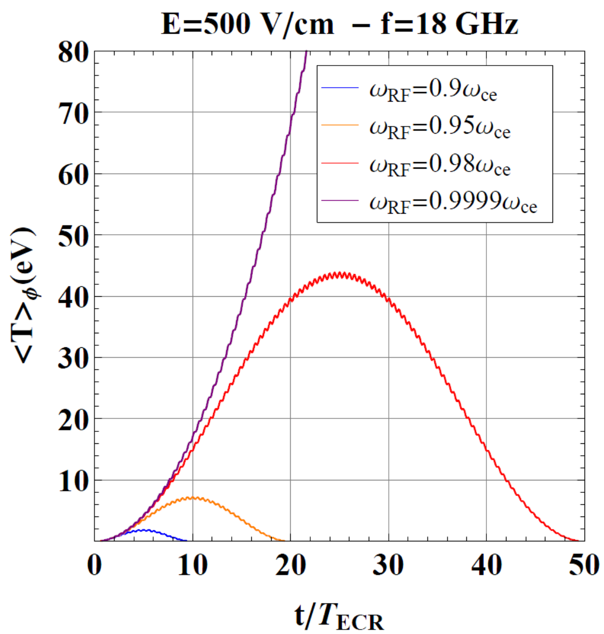

Figure 3: Evolution of the electron kinetic energy as a function of time for several values of $\Delta\omega$. The initial energy is taken as null here for convenience. The electron kinetic energy has a maximum as a function of time.

In order to build an estimator of the ECR frequency peak width, the maximum electron kinetic energy achievable T_{max} is plotted as a function of $\frac{\omega_{RF}}{\omega_{ce}}$ (see Fig. 4). The frequency width $\Delta\omega$ to be considered in Equation (5) is then the resonance width of the plot for a given kinetic energy allowing multi-ionization. One can note that the relative ECR peak width $\frac{\Delta\omega}{\omega}$ decreases with the ECR frequency. The reason is that the time to reach T_{max} is $t_{max} = \frac{\pi}{\Delta\omega}$, while on this plot the abscissa is $\frac{f_{RF}}{f_{ECR}} = 1 + \frac{\Delta\omega}{\omega}$. A fixed $\frac{f_{RF}}{f_{ECR}}$ ratio implies that $\Delta\omega \propto \omega$. Hence, $t_{MAX} \propto \frac{1}{\omega}$: for a given electrical field intensity and a given $\Delta\omega$, the higher the ECR frequency, the shorter the time for acceleration before an electron gets out phased, leading to a lower achievable kinetic energy. This study shows that the intrinsic ECR thickness is a constant independent of the ECR frequency. The phase averaged maximum of the electron kinetic energy for $\omega_{RF} = \omega_{ce} + \Delta\omega$ is:

$$T_{max} = \frac{2e^2}{m}\left(\frac{\omega_{ce}E}{\omega^2 - \omega_{ce}^2}\right)^2 + \frac{1}{2}m{v_0}^2 \cong \frac{e^2}{2m}\left(\frac{E}{\Delta\omega}\right)^2 \qquad (7)$$

provided $\frac{\Delta\omega}{\omega} \ll 1$ and $\frac{1}{2}m{v_0}^2 \ll \frac{e^2}{m}\left(\frac{E}{\Delta\omega}\right)^2$.

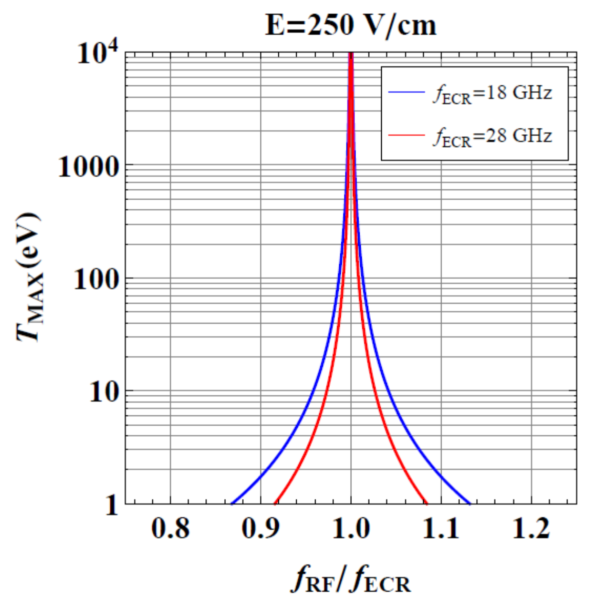

Figure 4: Evolution of the maximum kinetic energy that an electron can reach as a function of the RF frequency normalized to the ECR one, with an electrical field arbitrarily fixed to E=250 V/cm. The blue/red curves avec respectively the plots obtained for f_{RF}=18 and 28 GHz.

Model for the ECR Energy Boost per Passage

The Eq. 7 is eventually used to substitute $\Delta\omega$ in Eq. 5. This introduces the parameter T_{max} that is considered as a constant. In the following, a value of T_{max}~5 keV is considered to study the physics of ECR heating in the non-relativistic approximation. The energy kick per passage through the ECR zone is now:

$$\epsilon \sim \frac{eE^4}{4{v_{||}}^2 g^2 T_{max}} \qquad (8)$$

In the relativistic case, since the electron mass is γm, the resonance occurs on a different ECR surface, where $B \rightarrow \gamma B$, to keep the ECR condition $\omega_{ce} = \omega_{RF}$ valid. The study of $\Delta\omega = f(T_{max})$ can be extended by simulation to the relativistic case, when assuming that the magnetic field intensity automatically adjusts (by a factor γ) to the mass increase to match the ECR condition (gyrac effect). Simulation shows that the function $\Delta\omega = f(T_{max})$ does not change much in the relativistic case, apart from a relativistic boost occurring above ~10 keV. In the next

ISBN 978-3-95450-158-8

parts, the non-relativistic expression is assumed to represent the appropriate dimensional dependence of ϵ, even for relativistic electrons.

COMPARISON OF THE DATA WITH THE MODEL

The four magnetic configurations shown on Figure 1 have been simulated with RADIA and a 3 dimension magnetic field map was constructed.[4] For each configuration, the ECR zone is described by a network of $\sim 10^5$ points forming elementary surface triangles used to compute the magnetic gradient distribution over the ECR surface. A surface-weighted ECR gradient is next calculated. The ECR volume is estimated for each configuration on the basis of the ECR thickness:

$$\Delta l = \frac{m\Delta\omega}{eg} \cong \frac{\sqrt{m}E}{\sqrt{2T_{max}}\, g} \qquad (9)$$

An electrical field of 250 V/cm, and a kinetic energy $T_{max} = 5\,keV$ are used to estimate Δl. A summary of the ECR zone geometry is presented in Table 3 for the four VENUS plasma configurations presented in the first section of the paper.

Table 3: ECR zone geometry derived from the 4 magnetic configurations as on Fig. 1. Lengths, surfaces and volumes are expressed in cm, cm^2 and cm^3 respectively; magnetic gradients are in T/m.

	18 GHz Steep	18 GHz Shallow	28 GHz Steep	28 GHz Shallow
ECR Surface	530.3	389.8	519.2	382.8
ECR Thickness	3.5×10^{-3}	4.8×10^{-3}	2.2×10^{-3}	3.1×10^{-3}
ECR Volume	1.85	1.91	1.14	1.18
Min Gradient	6.7	5.1	10.4	8.0
Max Gradient	22.7	17.0	35.4	26.5
Mean Gradient	17.2	12.5	26.7	19.5

Shallow/Steep Gradient Comparison

For a given frequency (18 or 28 GHz), one can notice that increasing the axial gradient by reducing B_{min} increases greatly the ECR surface (by ~33-35%) but on the other hand it reduces the ECR thickness (by ~33-37%) which lets the ECR volume quasi unchanged. Because the RF power absorbed by the ECR mechanism is necessarily proportional to the ECR volume, it is reasonable to assume that the RF electrical field intensity is a constant for the two magnetic gradient configurations. It is thus possible to compare the mean energy boost ϵ for the two gradients and test the model presented earlier (see Table 4). It is noticeable that the ratio of the energy kick for the shallow and steep gradient closely fits the respective experimental x-ray temperature ratios. When the B_{min} value is changed, the electron energy boost closely fits with g^{-2}. So, in the framework of the simple electron heating model $W_\perp \sim N\epsilon$, the mean gain of electron energy is not due to a change of the electron confinement time, but mainly to a change in the ECR zone thickness. This result obtained was not obvious because the two magnetic gradients configurations have a significantly different axial magnetic mirror ratio which could have been thought as being able to modify the electron confinement time and thus the hot x-ray tail temperature.

Table 4: Comparison of experimental data with the model for a given ECR frequency

	18 GHz Steep	18 GHz Shallow	28 GHz Steep	28 GHz Shallow
ϵ (A.U.)	6.25	11.83	2.59	4.86
$\frac{\epsilon_{shallow}}{\epsilon_{steep}}$	1.89		1.87	
$\frac{kT_{shallow}}{kT_{steep}}$	1.91		1.89	

ECR Frequency Effect

The model developed to estimate the mean energy kick per passage ϵ through the ECR zone shows that the intrinsic ECR peak width $\Delta\omega$ is independent of the ECR frequency. Because in a given ECR ion source the magnetic gradient is increased proportionally to the ECR frequency ($g \propto f_{ECR}$), the ECR zone thickness goes like $\Delta l \propto 1/f_{ECR}$ and ϵ like f_{ECR}^{-2}. The comparison of the 18 and 28 GHz experimental results is not obvious because, as it can be seen in the table 2, the ECR volume scales with $1/f_{ECR}$, which implies that, for a given electrical field intensity, the total RF power absorbed by the ECR volume is $\propto 1/f_{ECR}$. So the equilibrium of the RF wave in the source cavity is different and one would expect a different quality factor Q of the cavity (the electromagnetic wave (EMW) being less absorbed per passage through the plasma, a larger number bounce in the cavity can be imagined for the wave). Thus, the electrical field to consider in the Eq. 8 is unlikely to be the same for different ECR frequencies.

If one assumes an equal electrical field intensity for both frequencies and a constant electron confinement time, the model of mean electron energy $W_\perp \sim N\epsilon$ scales like f_{ECR}^{-2}. But experimentally, we observe that the hot x-ray tail temperature is such that $kT \propto f_{ECR}$. Consequently, under this hypothesis, the discrepancy between the model and experimental measurements is proportional to f_{ECR}^{-3}. The only way for the model to match the experimental measurements is to assume that the confinement time scales with f_{ECR}^3, which is unlikely to be real.

ISBN 978-3-95450-158-8

If now one assumes that, for the same RF power injected, the electrical field intensity is changing with the RF frequency (because the power absorbed by the ECR mechanism in a magnetic gradient scales with f_{ECR}^{-1}), we can at least estimate the maximum theoretical electrical field reached in the cavity for a given ECR frequency. The RF power injected in the ion source can either be absorbed by the ECR zone (plasma), reflected or lost to the cavity wall:

$$P_{injected} = P_{ECR} + P_{reflected} + P_{wall} \qquad (10)$$

If we assume a perfect cavity wall and a null reflected power, one can consider the perfect case when all the RF is absorbed by the ECR mechanism:

$$P_{injected} = P_{ECR} \sim \frac{E_Q{}^2}{2\epsilon_0} V_{ECR} \propto \frac{E_Q{}^2}{2\epsilon_0} \frac{1}{f_{ECR}} \qquad (11)$$

Where $E_Q = QE$ is the RF field intensity in the cavity with a quality factor Q at the frequency f_{ECR} and E the original electrical field of the propagating RF wave in the section of the cavity. This leads to $E_Q{}^2 \propto f_{ECR}$. So in this theoretically perfect cavity, because $\epsilon \propto \frac{E^4}{g^2}$ we get, at best, $\epsilon(f_{ECR}) \sim Const$ and the energy per passage does not scale with the ECR frequency. So, in the case of a frequency increase, the model fit to the data implies that $W_\perp \sim N\epsilon \sim f_{ECR}$ which is only fulfilled if $N \propto f_{ECR}$: the higher energy x-ray observed are then understood as a consequence of a higher electron confinement time proportional to the ECR frequency, leading to higher energy electrons. This study is consistent with the explanation that the higher electron energies observed at higher ECR frequency are due to the electron RF scattering reduction expected by theory.[2]

SPATIAL GYRAC EFFECT

Another possible track for the high energy x-ray observed in ECRIS is the so-called spatial gyrac effect.[6] The ECRIS magnetic field structure is a minimum-B with field lines along which the magnetic intensity change is important. See for instance on Fig.1 the axial magnetic profile of VENUS where the axial field line evolves from $B_{max} = 3.4\,T$ down to $B_{min} = 0.5\,T$ for the 28 GHz steep gradient configuration, while the ECR is located at $B = 1\,T$. This extended magnetic gradient can favour a thick ECR condition for electrons propagating along a field line with an appropriate parallel velocity $v_{||}$ such that the relativistic mass increase (due to the perpendicular velocity increase) equals to the magnetic field increase:

$$\omega_{RF} = \frac{eB(t)\uparrow}{\gamma(t)m\uparrow} = Const \qquad (12)$$

In this case, an electron can reach a relativistic energy in a single passage through the magnetic gradient going from B_{ecr} to B_{max}. The maximum theoretical relativistic factor reachable when the electron goes up the magnetic mirror peak is $= B_{max}/B_{min}$. The calculation for the VENUS source heated at 28 GHz gives ~1.2 MeV which is consistent with what is experimentally observed in the x-ray energy spectrum. On the other hand, no ECR frequency effect is *a-priori* expected on the spatial gyrac effect in an ECRIS because the magnetic field structure is changed with a homothetic ratio leading to the same value of B_{max}/B_{min}.

REFERENCES

[1] D. Leitner, J. Y. Benitez, C. M. Lyneis, D. S. Todd,T. Ropponen, J. Ropponen H. Koivisto, and S. Gammino, Rev. of Scient. Instrum., 79, 033302 (2008).

[2] A. Girard, C. Pernot, and G. Melin, Phys. Rev. E, Vol. 62, No. 1, 2000, p.1182.

[3] C. Perret, A. Girard, H. Khodja, and G. Melin, Phys. Plasmas, Vol. 6, No. 8, 1999, p. 3408.

[4] RADIA, magnetic-field simulation code, © ESRF, Grenoble, France, portions © Wolfram Research Inc., http://www.esrf.fr/machine/groups/insertion_devices/Codes/Radia/Radia.html

[5] R. Geller, Electron Cyclotron Resonance Ion Sources and ECR plasmas, Institute of Physics Publishing, Bristol., CRC Press, 1996, p. 110.

[6] R. Geller, Electron Cyclotron Resonance Ion Sources and ECR plasmas, Institute of Physics Publishing, Bristol., CRC Press, 1996, pp. 112, 184.

ISBN 978-3-95450-158-8